

REVISTA BIO CIENCIAS http://revistabiociencias.uan.edu.mx

https://doi.org/10.15741/revbio.11.e1696_



Artículo original/Original Article

Healthy Snacks Made by Extrusion from Blue Corn (Zea mays L) and Amaranth (Amaranthus hypochondriacus L.)

Botanas Saludables Elaboradas por Extrusión a Partir de Maíz Azul (Zea mays L) y Amaranto (Amaranthus hypochondriacus L.)

Díaz, J. S⁶, Salomón-Montijo, B.* , Márquez-Salazar, G. , Gámez-Duarte, E. A

ABSTRACT

rupicolous-pendulous.

¹ Posgrado en Ciencias Biológicas, Facultad de Biología, Universidad Autónoma de Sinaloa. Ciudad Universitaria, Blvd. de las Américas y Blvd. Universitarios S/N. C. P. 80013, Culiacán Rosales, Sinaloa, México.

In May 2022, during a one-week exploration in the Sierra de Alica, La Yesca municipality, Nayarit, some cacti were collected. Disocactus speciosus subsp. speciosus, a genus and species not previously reported for the Nayarit flora, was recorded. The specimens were determined by specialists at the Biology Faculty of the Autonomous University of Sinaloa by reviewing specialized literature and matching specimens from the EACS-UAS herbarium. The species is rupicolous, pendulous, threeribbed stems, short spines on areoles with hirsute hairs, red polypetalous flowers, numerous stamens, and cream-colored feathery stigma, the fruit is an ovoid berry covered with spiny, caedaceous areoles, edible at maturity. The record complements the distribution of the genus and the species in an entity located between two states that already have it inventoried in their flora.

KEY WORDS: Sierra de Alica, mixed pine-oak forest,

Cactaceae, polypetalous red flowers, rupicolous-pendulous,



Please cite this article as/Como citar este artículo: Díaz, J. S., Salomón-Montijo, B., Márquez-Salazar, G., Gámez-Duarte, E. A. (2024). First record of Disocactus speciosus (Cav.) Barthlott subsp. speciosus (Cactaceae: Cactoideae) In Nayarit, Mexico. Revista Bio Ciencias, 11,

https://doi.org/10.15741/revbio.11.e1696

Article Info/Información del artículo

Received/Recibido: April 17th 2024. Accepted/Aceptado: October 03th 2024. Available on line/Publicado: October 24th 2024.

*Corresponding Author:

Bladimir Salomón-Montijo. Facultad de Biología, Universidad Autónoma de Sinaloa. Ciudad Universitaria, Blvd. de las Américas y Blvd. Universitarios S/N. C. P. 80013, Culiacán Rosales, Sinaloa, México. Tel. (+52)667 716 1139. Email: vladimir.salomon@uas. edu.mx



RESUMEN

En mayo de 2022 durante una exploración de una semana en la Sierra de Álica, municipio de La Yesca, Nayarit, se colectaron algunas cactáceas. Se registró Disocactus speciosus subsp. speciosus, un género y especie no reportados previamente para la flora nayarita. Los especímenes fueron determinados por especialistas en la Facultad de Biología de la Universidad Autónoma de Sinaloa mediante revisión de literatura especializada y el cotejo de especímenes del herbario EACS-UAS. La especie es rupícola, péndula, tallos de tres costillas, espinas agudas en aréolas con pelillos hirsutos, flores polipétalas rojas, estambres numerosos, estigma plumoso color crema, el fruto es una baya ovoide cubierta de areolas espinosas caedizas, comestible en la madurez. El registro complementa la distribución del género y la especie en una entidad ubicada entre dos estados que ya la tienen inventariada en su flora.1

PALABRAS CLAVE: Sierra de Álica, bosque mixto de pino-encino, Cactaceae, flores rojas polipétalas, rupícola-péndula.

Introduction

Second-generation snacks are consumed between meals to provide satiety, entertainment, or satisfy the consumer's taste. However, most products of this type are made from corn starch or starch-rich corn fractions and additives such as sugars and fats. The abovementioned results in poor nutritional quality and a high caloric content. Due to this, snacks have been associated with the prevalence of malnutrition, which is an undesirable physical condition caused by the lack or excess of nutrients, as well as the incidence of obesity and chronic degenerative diseases such as diabetes mellitus, fatty liver, and certain types of cancer (Shah *et al.*, 2018).

Nowadays, there has been growing interest in the use of whole grains as raw materials for the development of high-consumption food products (such as tortillas, snacks, pasta, etc.) with good nutritional and nutraceutical value that offer health benefits and help to prevent chronic degenerative diseases, such as bioactive compounds with antioxidant potential. Additionally, emerging technologies (innovative or developing technologies that need to be investigated to assess their social, economic, and environmental impact, as well as their possible improvements and solutions) are being implemented in food production to preserve or transform certain nutrients and compounds with antioxidant activity. One widely technology used in the expanded snacks production is extrusion. Extrusion is a process where food pass through simultaneous shearing, mixing, and cooking operations, causing various transformations, such as protein denaturation, starch gelatinization, lipid oxidation, degradation of vitamin and antioxidant compounds, or



even the generation of the latter (Leonard *et al.*, 2019). Previously, Félix *et al.* (2021) produced expanded snacks through extrusion using corn and beans, obtaining a nutritionally improved product due to the increased protein content, complementation of essential amino acids, and improved protein digestibility, along with antioxidant properties that could reduce the prevalence of chronic degenerative diseases (Herrera *et al.*, 2017). On the other hand, Espinoza *et al.* (2016) produced snacks through extrusion using transgenic corn and common black beans, obtaining a product with higher protein, fiber, and phenolic compound content compared to similar commercial snacks.

Corn is one of the most widely used sources of starch in research and the food industry. Blue corn stands out compared to other grains or corn varieties due to its high fiber content, vitamins, essential amino acids, and compounds with antioxidant properties. This makes it an excellent raw material for snack-type products (Escalante et al., 2014; Herrera et al., 2017). However, corn is deficient in lysine and tryptophan, making it necessary to complement using other grains rich in these essential amino acids to increase their content in the grain mixture. This approach helps meet the essential amino acid requirements that proteins must fulfill according to FAO standards. According to previous reports, amaranth possesses a high lysine and tryptophan content. Moreover, this pseudocereal is also a rich source of vitamins, minerals, and phytochemicals (USDA, 2018; Soriano et al., 2019). However, the inclusion of this grain may affect the sensory and techno-functional characteristics of the final product, making it necessary to optimize process variables to obtain an expanded snack with high antioxidant value and protein digestibility, as well as appropriate physical and textural characteristics for a second-generation snack. Based on the above, the objective of this research was to optimize the extrusion conditions and the blue cornamaranth ratio to develop an expanded snack with good antioxidant properties, phytochemical content, protein digestibility, and texture, using whole-grain mixtures of blue corn and amaranth.

Material and Methods

Materials

Blue corn (*Zea mays* L.) and amaranth (*Amaranthus hypochondriacus* L.) were obtained from the National Institute of Forestry, Agricultural, and Livestock Research (INIFAP) in Celaya, Guanajuato, Mexico, and from a market in Temoac, Morelos, Mexico, respectively. Additionally, the following reagents and solvents were used: sodium hydroxide (NaOH), hydrochloric acid (HCl), ethanol (C_2H_6O), methanol (C_3OH), hexane (C_6H_{14}), ethyl acetate ($C_4H_8O_2$), sodium carbonate (C_2C_3), Folin-Ciocalteu reagent, gallic acid, sodium nitrite (C_3C_3), aluminum chloride (AlCl₃), potassium persulfate ($C_3C_3O_3$), 2,2'-azino-bis(3-ethylbenzothiazoline-6-sulfonic acid) ($C_3C_3C_3$), monobasic potassium phosphate ($C_3C_3C_3$), disodium phosphate anhydrous ($C_3C_3C_3$), pepsin, pancreatin, trichloroacetic acid ($C_3C_3C_3$), potassium sulfate ($C_3C_3C_3$), copper sulfate ($C_3C_3C_3$), sulfuric acid ($C_3C_3C_3$), and casein. All reagents were purchased from Macerlab in Culiacán, Sinaloa.



Methods

Sample preparation and acquisition

In this research, snacks were developed using whole grains of blue corn, amaranth, and water. Any additional ingredients were employed. Blue corn and amaranth grains were ground into flours (#40 mesh, 0.425 mm). The flour mixture was prepared with different proportions of amaranth flour (AF) = 0 - 70%, and conditioned to obtain 18% moisture by adding purified water. Extrusion was performed using a single-screw extruder, model 20 DN (CW Brabender Instruments, Inc, NJ, USA), with a screw diameter of 19 mm, a length-to-diameter ratio of 20:1, a nominal compression ratio of 3:1, and a 5 mm die opening. Different barrel temperatures (BT) = 120 - 170 °C and screw speeds (SS) = 50 - 240 rpm were used (Félix *et al.*, 2020). The expanded extruded snacks (EES) were collected and packaged to evaluate three quality characteristics: radial expansion index (REI), apparent density (AD), and hardness (H). Subsequently, the extrudates were air-dried and ground in a hammer mill (LM 3100, USA) until they passed through an #80 mesh (0.180 mm). Four properties were analyzed on the resulting flours: antioxidant activity (AoxA), total phenolic content (TPC), total flavonoids (TF), and *in vitro* protein digestibility (IVPD).

Evaluation of Response Variables

Radial expansion index (REI), apparent density (AD), and hardness (H)

The expanded snacks were cut into samples of 5 cm in length, and 10 were randomly selected to measure diameter and weight. The REI value was obtained by dividing the diameter of the expanded snack by the die opening of the extruder (Gujska & Khan, 1990), and the AD value was obtained using the following equation (Wang *et al.*, 1993):

Equation 1

Where: sw = sample weight (g), = average diameter of the sample (cm), and = length of the sample (cm).

For hardness (H) determination, the technique described by Park *et al.* (1993) was employed. A Universal Texture Analyzer Model 4411 with a 1 mm diameter probe was used to measure the force required to penetrate 60 % of the expanded snack. The measurement conditions were: Load of 500 kg for penetration and a speed of 2 mm/s. A total of 90 hardness measurements were performed.

Content of phytochemicals and antioxidant activity

Obtention of free and bound phenolic extracts

The free phenolics extraction was performed by suspending 0.5 g of the sample in 10 mL



ethanol and water (80:20 %, v/v) (Dewanto *et al.*, 2002). The suspended sample was stirred in a rotary tube homogenizer (50 rpm, 10 min), then centrifuged (8,000 rpm, 10 °C, 10 min), and the remaining pellet was subjected to a second extraction. The supernatants from the two extractions were concentrated at 45 °C using a low-pressure concentrator (Apud Vac Concentrator, Thermo Electron Corporation), and the recovered extracts were evaporated at 45 °C (1 - 2 nights) and stored at -20 °C. The sediments obtained after the extraction of free phenolic compounds were defatted with hexane and then hydrolyzed with 10 mL of NaOH (2 M) at 95 °C and 25 °C for 30 and 60 minutes, respectively. The hydrolyzed extract was neutralized with HCI. The bound phenolic extracts were obtained through four extractions with 10 mL of ethyl acetate (Adom & Liu, 2002; Adom *et al.*, 2003). The extracts were evaporated and stored until use. The extractions of phenolic compounds were performed in quadruplicate.

Total phenolic content

For the determination of total phenolic content (TPC), a standard solution of gallic acid was prepared. A 20 μ L aliquot of the standard solution (25 - 600 ppm) and the phenolic extracts (free and bound) were injected into a 96-well microplate. Each point of the standard curve and extract reacted with 180 μ L of Folin-Ciocalteu reagent and 50 μ L of a 7 % Na₂CO₃ solution and was incubated at 25 °C for 90 minutes. The absorbance of the samples was read at 750 nm using a Multiskan Skyhigh microplate reader (Thermo Scientific, Singapore) with methanol as the blank. The TPC results were calculated by summing the phenolic compounds in the free and bound extracts and expressed as mg gallic acid equivalents (GAE) per 100 g of dry sample (Singleton *et al.*, 1999). The determinations were performed in quadruplicate.

Total flavonoid content

The determination of total flavonoids (TF) was performed using the colorimetric assay described by Xu & Chang (2007). A mixture of 20 μ L of the extract and 80 μ L of distilled water was prepared. Then, 6 μ L of NaNO₂ and 12 μ L of AlCl₃ were added, allowing the mixture to rest for 5 minutes after each reagent. Finally, 40 μ L of a 1 M NaOH solution and 20 μ L of distilled water were added. The mixture was left to rest for 30 minutes, and the absorbance was read at 415 nm using a Multiskan Skyhigh microplate reader (Thermo Scientific, Singapore). Quercetin was used as the standard in the calibration curve. The determinations were performed in quadruplicate, and the results were calculated and expressed as mg quercetin equivalents (QE) per 100 g of dry sample.

Antioxidant activity

The antioxidant activity was determined using the decolorization assay described by Re et al. (1999). An ABTS solution was prepared by mixing 0.0192 g of the radical with 5 mL of 2.45 mM $\rm K_2S_2O_8$, and the mixture was left to rest for 16 hours in darkness. Then, 500 $\rm \mu L$ of the ABTS solution was diluted in 45 mL of phosphate-buffered saline (PBS) (pH 7.4), and its absorbance was adjusted to 0.7 - 1.0 at 734 nm. Once the absorbance of the radical was adjusted, 1980 $\rm \mu L$ of the adjusted radical was added to 20 $\rm \mu L$ of the extract, and its absorbance was read at 734 nm after 6 minutes using a Multiskan Skyhigh reader (Thermo Scientific, Singapore). The determinations



were performed in quadruplicate, and the results were expressed as µmol Trolox equivalents (TE) per 100 g of dry sample.

In vitro protein digestibility

In vitro protein digestibility (IVPD) was determined using the procedure described by Rathod *et al.* (2016) with modifications. One gram of the sample was incubated for 3 hours with 15 mg of pepsin in 20 mL of HCI (0.1 N) at 37 °C in a water bath with moderate agitation. After the incubation period, the sample was neutralized by adding 10 mL of NaOH (0.2 N), and the pH was adjusted to 8.0. Then, 40 mg of pancreatin in 7.5 mL of PBS (pH 8.0) was added, and the mixture was left to rest at 37 °C for 24 hours with moderate agitation. At the end of the incubation period, 700 μ L of trichloroacetic acid was added. The sample was washed with distilled water, and centrifuged at 5,000 rpm for 10 minutes, and the precipitate was dried at 45 °C and used for protein quantification (MicroKjeldahl method). The determinations were performed in triplicate, using casein as a control, and IVPD values were calculated with the following equation:

Equation 2

Experimental design, statistical analysis, and optimization

For the optimization of the extrusion process conditions and the percentage of amaranth in the snack, a central composite rotatable experimental design was used with three process variables: extrusion temperature (BT, 120 - 170 °C), screw speed (SS, 50 - 240 rpm), and amaranth flour percentage (AF, 0 – 70 %). The minimum and maximum values of SS were selected based on the characteristics of the extruder, which operates within a range of 50 - 240 rpm. In contrast, the minimum and maximum values of BT and AF were selected through a literature review and preliminary trials. In the literature review and preliminary trials, it was found that BT values above 120 °C are necessary to achieve acceptable expansion (similar to commercial products) in this type of snack, and values above 170 °C cause flow problems of the sample within the extruder, leading to equipment blockage and adhesion of the sample inside the extruder. To vary the levels of amaranth flour in the blue corn-amaranth mixtures, the article published by Félix et al. (2020) was taken as a reference; they varied the inclusion level of beans from 0 - 70 % in different cornbean mixtures to optimize the conditions for obtaining a second-generation snack using a singlescrew extruder. The purpose of varying AF during optimization was to study the effect of including different amounts of amaranth flour in blue corn-amaranth mixtures on the physical, textural, antioxidant, and protein digestibility properties of second-generation snacks. Low (0 %) and high (70 %) AF inclusion values were selected in the blue corn-amaranth mixture to fit appropriate and reproducible second-order regression models for each response variable. A wide range of AF (0 - 70 %) in the blue corn-amaranth mixture allowed an extensive range of variability in the analyzed responses, ensuring better mathematical regression models. In contrast, a narrower AF inclusion range in the mixtures would have decreased the likelihood of obtaining adequate regression models for all the studied responses. The response variables evaluated were radial expansion index (REI), apparent density (AD, g/cm³), hardness (H, N), total phenolic content (TPC, mg GAE / 100 g, dw), total flavonoid content (TF, mg QE / 100 g, dw), antioxidant activity



(AoxA, µmol TE / 100 g, dw), and in vitro protein digestibility (IVPD, %). Once the results of the response variables under different process conditions were obtained, the relationship between the independent variables (BT, SS, and AF) and the dependent variables (REI, AD, H, TPC, TF, AoxA, and IVPD) was analyzed through multiple linear regression by least squares using the software Design Expert version 11.1.2.0. Seven prediction models were obtained, and each model was used to represent the effect of the process variables on their respective response variable through response surface plots. Additionally, the stationary point coordinates for each response variable were obtained, and if the stationary point was within the experimental range, a characterization of the response surface was performed through canonical analysis, where the eigenvalues or characteristic roots (\lambda) were determined. Furthermore, the nature of the response surface was determined based on the stationary point and the signs and magnitudes of all the eigenvalues. The stationary point represents a minimum response if all eigenvalues are positive, a maximum response if all eigenvalues are negative, and a saddle point if the eigenvalues have different signs. To find the maximum and minimum values within the experimental region, single-response optimization was performed using the desirability method via Minitab version 19 software. These results were also validated using the ridge analysis method of response surface methodology (Gutiérrez and De la Vara, 2008; Khuri and Mukhopadhway, 2010). Subsequently, the numerical desirability method for multiple responses was applied using Design Expert version 11.1.2.0 to find the combination of process variables that allowed the maximization of REI, AoxA, TPC, TF, and IVPD values, and the minimization of AD and H. From the numerical desirability method, the individual desirability degree (d) for each response variable was found, and the global desirability (D) was obtained using the following equation:

Equation 3

Where the ideal value is D = 1, and an acceptable desirability value for food systems can be found between 0.6 and 0.8.

Results and Discussion

Experimental results and multiple linear regression analysis

The experimental values obtained for each response variable under different process conditions are shown in Table 1. Average values and standard deviations are not presented in this experimental design because the treatments were conducted only once (no replicates). Only the central treatment (145 °C, 145 rpm, 35 % AF) was performed six times (six replicates); however, Table 1 includes the response variable values corresponding to each of the six replicates. Additionally, the minimum and maximum values for each process variable and response variable are highlighted.

On the other hand, Table 2 shows the results obtained from the linear regression for the different response variables. The β values represent the intercept coefficients and the linear, quadratic, and interaction terms of the mathematical prediction models with coded variables for



each response variable. The signs and magnitudes of the β coefficients indicate the effect of the corresponding term on the response variable. Negative signs mean that the term causes decreases in the response, while positive signs lead to increases. Furthermore, it is observed that the regression models are significant (p < 0.0001), with adjusted determination coefficients (R_{adi}^2) ranging from 0.8530 to 0.9730, and they do not show a lack of fit (p > 0.05). It is worth mentioning that a good prediction model exhibits a statistical significance level of p-model ≤ 0.05, an adjusted determination coefficient $R^2 \ge 0.80$, a lack of fit value p > 0.05, and a coefficient of variation CV ≤ 10 %. Therefore, the statistical parameters presented in Table 2 demonstrate that the obtained polynomial models fit the experimental behavior shown by the evaluated response variables. The mathematical models obtained for each response variable include significant linear, quadratic, and interaction terms (p < 0.05). However, some non-significant terms were included to achieve better fitting parameters. In the AD variable, the interaction term between BT and AF was included; in the H variable, the linear SS term was included; and in the AoxA variable, the linear terms of BT and SS and the guadratic term of SS were included. Furthermore, in Figures 1 and 2, the response surface plots obtained for each response variable as a function of BT, SS, and AF are shown. These three-dimensional graphs allow the analysis of the response variable (Y-axis) as a function of only two process variables (X, and X, axes); therefore, in this case, one process variable needs to be fixed. In our case, on a fourth axis (X3), three values of the third process variable were fixed to observe the effect of the three variables selected for this study. BT and AF were subjectively selected for the X_1 and X_2 axes, respectively. These process variables were chosen to observe their effect on the behavior of the response variables. Meanwhile, the vertical axis Y represents the response variable. SS was selected to set three values on the horizontal axis (X2) because it was the process variable with the lowest effect on most response variables. The three values chosen for the SS variable were the axial (50 and 240 rpm) and central (145 rpm). This criterion was established for all graphs to provide a better perspective for interpreting the graphical behavior of the different response variables.

REI had minimum and maximum values of 1.857 and 2.327 (Table 1), respectively. Additionally, it can be observed in Figure 1A that an increase in REI is mainly caused by decreases in BT and AF. On the other hand, increased SS allows REI values to rise. In Table 2, it can be observed that BT has a potent effect on REI, while the linear term of AF did not have a significant effect. Likewise, REI was affected by the quadratic term of SS and the interactions BT-SS and BT-AF. Additionally, response optimization revealed that the maximum desirable value of REI (2.42) is found at BT = 120 °C, SS = 205.5 rpm, and AF = 0 %. Moreover, the stationary point coordinates were calculated (BT = 112.87 °C, SS = 262.23 rpm, AF = 109.48 %), and the BT, SS, and AF values are outside the experimental range, making it impossible to draw inferences about this point.

On the other hand, AD had minimum and maximum values of 0.178 and 0.473 g/cm³ (**Table 1**), respectively. **Figure 1B** shows that AD values consistently decrease as BT increases and AF decreases, meaning that minimum AD values are found at high BT values and low AF values. Additionally, SS did not have a significant effect on AD, so this response variable shows the same graphical behavior at different SS values. Moreover, this variable does not present a stationary point, as the model exhibits a linear behavior (**Table 2**) where AD is negatively affected



by BT (higher BT results in lower AD) and positively by AF (higher AF results in higher AD) in equal magnitude, as well as by the interaction between BT and AF.



Table 1. Experimental design used to produce expanded extruded snacks (EES) at different process conditions and experimental results of response variables evaluated in the EES.

Treatment1	Process conditions			Physica	Physical responses			eutical res	Nutritional response	
	ВТ	SS	AF	REI	AD	Н	TPC	TF	AoxA	IVPD
1	130.1	88.5	14.2	2.227	0.339	30.38	200	227	3397	27.3
2	159.9	88.5127	14.2	1.857	0.197	8.24	350	166	3400	55.0
3	130.1	201.4	14.2	2.327	0.364	32.78	318	239	2265	25.9
4	159.9	201.4	14.2	2.077	0.178	10.33	383	306	4049	66.4
5	130.1	88.5	55.8	2.173	0.455	33.29	201	93	2392	38.7
6	159.9	88.5	55.8	1.920	0.324	22.63	242	250	1525	35.5
7	130.1	201.5	55.8	2.273	0.422	34.03	278	21	1807	35.3
8	159.9	201.5	55.8	2.080	0.352	24.26	103	271	1756	47.7
9	120	145	35	2.303	0.470	38.14	267	202	2727	27.0
10	170	145	35	1.930	0.238	8.16	302	405	2868	63.8
11	145	50	35	1.931	0.398	24.32	321	194	3091	40.6
12	145	240	35	2.213	0.295	22.52	240	138	2869	54.8
13	145	145	0	2.126	0.204	12.52	285	77	3575	30.6
14	145	145	70	2.100	0.473	36.88	106	153	1147	36.9
15	145	145	35	2.080	0.378	27.87	267	172	2340	42.3
16	145	145	35	2.173	0.385	26.76	278	195	2374	39.9
17	145	145	35	2.153	0.295	20.47	275	165	2803	52.9



18	145	145	35	2.111	0.339	21.51	304	179	2835	49.5	
19	145	145	35	2.150	0.291	26.52	290	137	2865	45.7	
20	145	145	35	2.160	0.360	25.47	288	141	2686	38.8	

¹ Rotable composite central experimental design with three factors and five coded levels of variation; 20 experiments. AF = Amaranth Flour (%), BT= Barrel temperature (°C), SS = Screw Speed (rpm), REI = Radial Expansion Index, AD = Apparent Density (g/cm³), H = Hardness (N), TPC = Total Phenolic Compounds (mg GAE / 100 g, dw), TF = Total Flavonoids (mg QE / 100 g, dw), AoxA = Antioxidant Activity (μmol TE / 100 g, dw), *IVPD* = *In vitro* Protein Digestibility (%) * The bolded values of the process and response variables correspond to the minimum and maximum values used and obtained, respectively.

Table 2. Results of the regression analysis of polynomial models for the response variables studied.

	Regression parameter coefficients								
Parameters	Physical re	sponses		Nutraceutica	ıl responses	Nutritional response			
	REI	AD	Н	TPC	TF	AoxA	IVPD		
Intercept									
β0	2.13	0.3378	24.35	285.26	165.23	2672.93	45.56		
Linear									
β1	-0.1240***	-0.0675***	-8.45***	10.32***	55.05***	81.12NS	10.20***		
β2	0.0772***	NS	0.2812NS	-23.98***	-16.54*	-88.74NS	3.12**		
β3	NS	0.0678***	7.24***	-53.50***	22.55**	-711.21***	NS		
Quadratic									
β11	NS	NS	NS	NS	48.98***	NS	NS		
β22	-0.0186**	NS	NS	NS	NS	84.20NS	NS		
β33	NS	NS	NS	-29.83***	-17.73***	-134.58**	-4.16***		



Continuation							
β123	NS	_ NS	NS	-16.26***	NS	-120.53*	NS
β23	NS	NS	NS	-26.53***	-25.27***	NS	NS
β13	0.0216**	0.0157NS	3.02***	-43.65***	50.03***	-338.02***	-7.36***
β12	0.0225**	NS	NS	-37.53***	27.59***	324.61***	3.54**
Interactions							

Regression parameter coefficients

0.8530

0.8367

0.8261

9.91

Parameters	Physical re	esponses		Nutraceutica	al responses	Nutritional response	
	REI	AD	Н	TPC	TF	AoxA	IVPD
β112	NS	NS	NS	35.22***	29.04**	NS	NS
β113	NS	NS	-3.18**	NS	-60.41***	NS	NS
β122	NS	NS	NS	NS	NS	NS	NS
P-value for mode	I < 0.0001	< 0.0001	< 0.0001	< 0.0001	< 0.0001	< 0.0001	< 0.0001
	0.9642	0.8762	0.9600	0.9879	0.9784	0.9618	0.9061

0.9770

0.9364

0.9028

4.01

0.9544

0.9352

0.9252

9.64

0.9339

0.9139

0.9208

6.98

0.8726

0.8350

0.9384

9.75

0.9457

0.9445

0.9859

8.61

NS Not significant (p > 0.1), * Significant at p < 0.1, ** Significant at p < 0.05, *** Significant at p < 0.01, REI = Radial Expansion Index, AD = Apparent Density (g/cm³), H = Hardness (N), TPC = Total Phenolic Compounds (mg GAE / 100 g, dw), TF = Total Flavonoids (mg QE / 100 g, dw), AoxA = Antioxidant Activity (μ mol TE / 100 g, dw), μ IVPD = In vitro Protein Digestibility (%).

P-value for lack 0.8577

of fit CV (%) 0.9514

0.9353

1.34



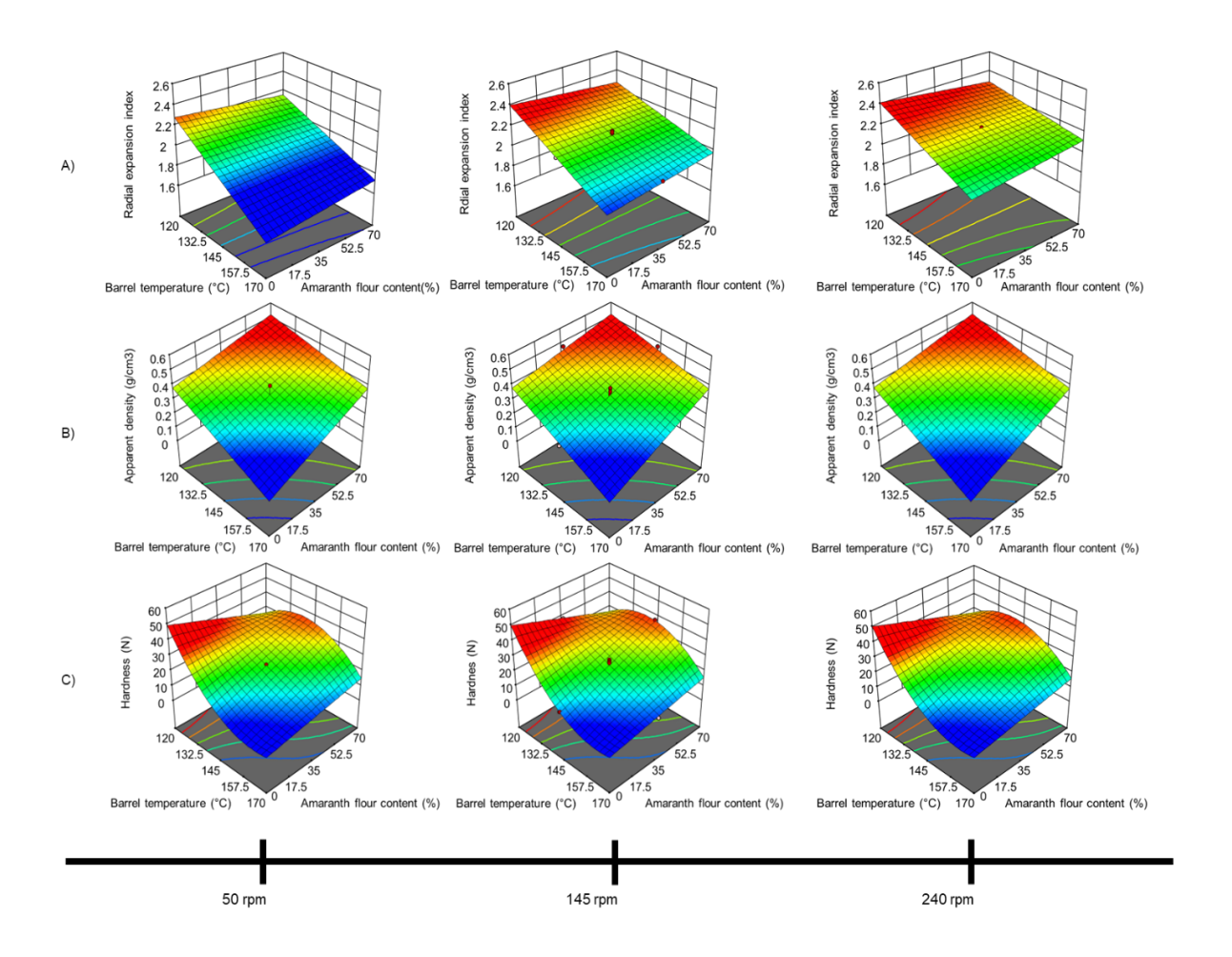


Figure 1. Response surface plots showing the effect of the extrusion process variables (Barrel Temperature, Amaranth Flour Content, Screw Speed) on the response variables (A) Radial Expansion Index, (B), Apparent density, (C) Hardness of expanded snacks produced from blue corn/amaranth flours mixtures.

Furthermore, response optimization revealed that the minimum desirable value of AD (0.066 g/cm³) was located at BT = 170 °C, AF = 0 %, and any SS value. This type of behavior is consistent with the findings of Gómez *et al.* (2021), who reported that an increase in BT causes greater expansion and, in turn, a reduction in AD due to a higher pressure gradient at the extruder outlet, which allows a higher level of starch gelatinization. Similarly, Nikinmaa *et al.* (2023) noted that expansion during extrusion can occur both radially and longitudinally, suggesting that the reduction in density, despite the decrease in radial expansion at high BT values, could be attributed to an increase in longitudinal rather than radial expansion, as was evaluated in the present study. On the other hand, the increase in AF adds fiber and proteins to the product, which compete with the starch for water and cause expansion issues (Félix *et al.*, 2020).



H had minimum and maximum values of 8.16 and 38.14 N (Table 1), respectively. Figure 1C shows that the minimum H values are located at high BT and low AF, which is consistent with previous findings (Félix *et al.*, 2020). Additionally, it can be seen that BT and AF exhibit a synergistic (interaction) effect. Increases in AF at low BT values reduce H, while increases in AF at high BT values increase H. Furthermore, Table 2 shows that H was negatively affected by BT; meanwhile, AF had a positive (undesirable) effect on this variable. The increase in radial and/or longitudinal expansion caused by the extrusion temperature is also related to an increased product porosity, which leads to lower H values. It is important to note that SS did not have a significant effect on H. The coordinates of the stationary point were calculated (BT = 109.36 °C, SS = 172.97 rpm, AF = 93.23 %), and it was found that the BT and AF values are outside the experimental range, making it impossible to draw inferences about this point. Moreover, response optimization revealed that the minimum desirable H value (4.55 N) was located at BT = 170 °C, AF = 0 %, and any SS value.

TPC values ranged from 103 to 383 mg GAE / 100 g (dw). Out of the total phenolic compounds, 3.97 - 30.88 % corresponded to free phenolic compounds and 69.12 - 96.03 % to bound phenolic compounds. Additionally, Figure 2A shows that TPC reached maximum values under intermediate BT and AF conditions and low SS. As SS increased, two points with maximum TPC values emerged, corresponding to (1) low BT and high AF, and (2) high BT and low AF, due to the synergistic effect between BT, SS, and AF. The interactions BT-AF, BT-SS, and BT²-SS had the greatest impact on this variable. Various authors mention that high SS values allow greater release of phenolic compounds bound to the cell wall. Moreover, an increase in BT activates Maillard reactions, producing compounds that can be detected at the same wavelength as phenolic compounds (Espinoza *et al.*, 2016; Félix *et al.*, 2020). Additionally, the coordinates of the stationary point were calculated (BT = 118.46 °C, SS = 102.62 rpm, AF = 53.35 %), and it was found that the BT value is outside the experimental range, making it impossible to infer about this point. Moreover, response optimization revealed that the maximum desirable TPC value (605 mg GAE / 100 g, dw) was located at BT = 170 °C, SS = 240 rpm, and AF = 0 %.

TF (Total Flavonoids) values ranged from 21 to 405 mg QE / 100 g (dw) (Table 1). In Figure 2B, it can be observed that at low SS values, a maximum TF value is found at low BT and AF, while a minimum value appears at low BT and high AF. However, as SS increases, the maximum TF value shifts positively, and a new high TF zone emerges at high BT and low AF. Finally, when SS reaches its highest value within the experimental range (240 rpm), two peaks are observed at the minimum and maximum BT values and the minimum AF value. This behavior is due to the same release and transformation mechanisms previously mentioned for TPC. Additionally, the increase in AF causes a reduction in both TPC and TF, as amaranth has a lower content of phenolic compounds and flavonoids compared to blue corn (Gámez et al., 2021). Moreover, Table 2 indicates that the three process variables, BT, SS, and AF, had a statistically significant effect on TF, with BT being the most influential variable. The interactions were statistically significant in the following order: BT-AF, BT-SS, BT2-SS, SS-AF, and BT-SS-AF. The coordinates of the stationary point were calculated (BT = 163.57 °C, SS = 113.76 rpm, AF = 36.25 %), and it was found that the BT, SS, and AF values are within the experimental range. Additionally, the results of the response surface characterization (λ_1 = 2.68, λ_2 = -23.48, λ_3 = 52.05) show that the stationary point is a saddle point, and the surface exhibits a steeper slope in the direction of w₃ (the transformed



independent variable corresponding to AF), where the absolute value of λ_3 had the maximum value. Furthermore, the optimization revealed that the maximum desirable TF value (714 mg QE / 100 g, dw) is located at BT = 170 °C, SS = 240 rpm, and AF = 0 %.

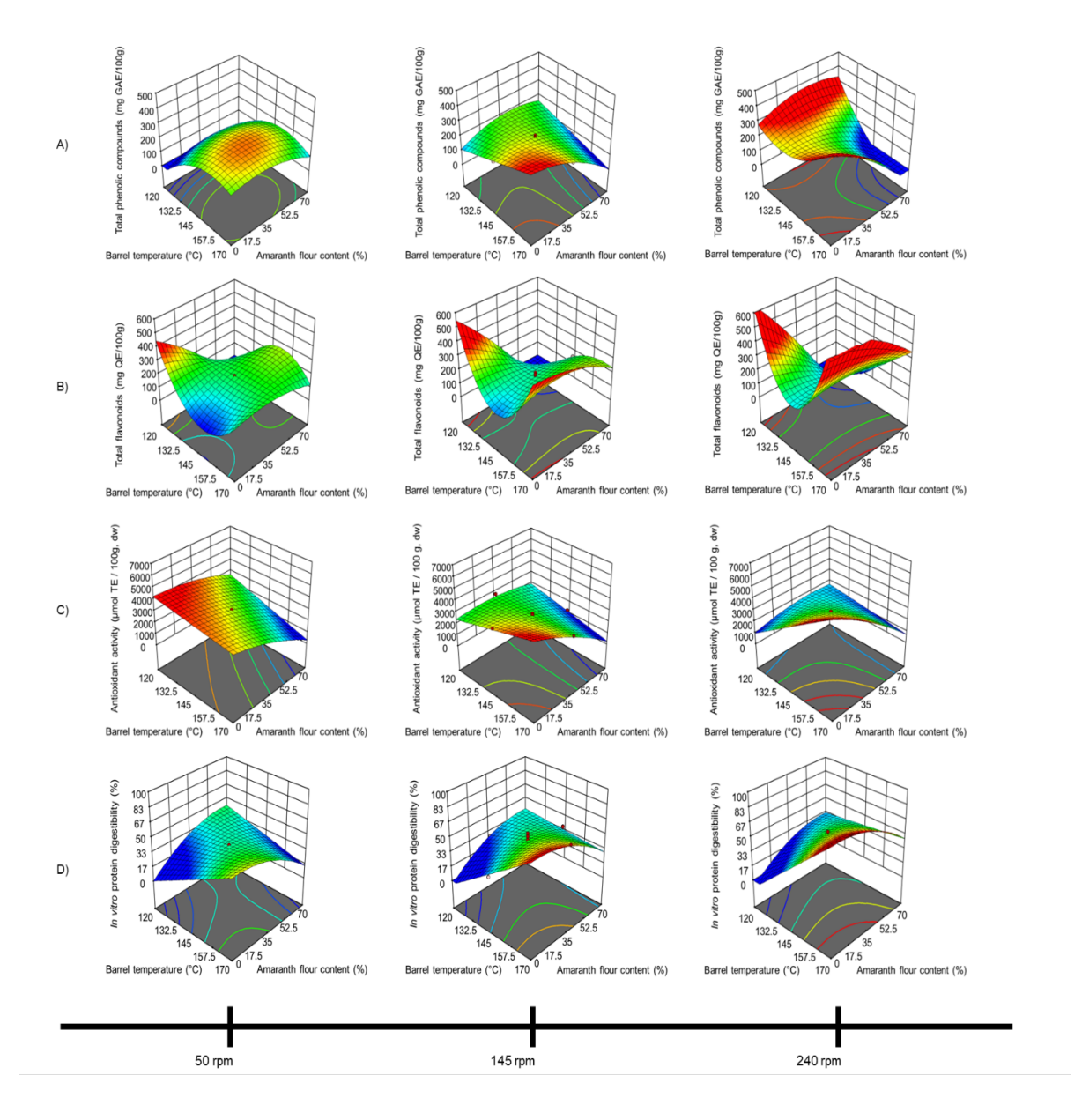


Figure 2. Response surface plots showing the effect of the extrusion process variables (Barrel Temperature, Amaranth Flour Content, Screw Speed) on the response variables (A) Total Phenolic compounds, (B) Total flavonoids, (C) Antioxidant activity, (D) *in vitro* protein digestibility of expanded snacks produced from blue corn/amaranth flours mixtures.



AoxA presented values between 1147 - 4049 µmol TE / 100 g (dw) (Table 1). Figure 2C shows that, at low SS values, there is a loss of AoxA with the increase of BT and AF. However, as SS increases, the maximum value of AoxA shifts toward higher BT values. In contrast, the minimum AoxA value is at high BT and AF values for any SS value. On the other hand, Table 2 indicates that AoxA was mainly affected by AF, while the linear terms of BT and SS did not show a significant effect on AoxA. However, the quadratic term of AF and the interactions between BT-SS, BT-AF, and BT-SS-AF had a substantial effect on it, making it clear that the values of this response variable will be affected by changes in both BT and SS, as well as AF. High SS values allow a higher release of compounds with antioxidant activity from the cell wall. Additionally, high BT activates reactions that produce compounds with antioxidant activity and inactivates enzymes, preventing the oxidation of some phenolic compounds (Félix et al., 2020). Likewise, it has been reported that amaranth shows lower antioxidant activity compared to blue corn (Gámez et al., 2021). Moreover, the stationary point coordinates were calculated (BT = 112.41 °C, SS = 174.77 rpm, AF = 50.53 %), and it was found that the BT value is outside the experimental range. Additionally, the optimization of a variable revealed that the maximum desirable value of AoxA (6161 µmol TE / 100 g, dw) is located at BT = 170 $^{\circ}$ C, SS = 240 rpm, and AF = 0 %.

The minimum and maximum IVPD experimental values obtained were 25.9 and 66.4 % (Table 1), respectively. In Figure 2D, it can be observed that for any SS value, the minimum value is located at low BT and AF; meanwhile, the maximum value is located at high BT and low AF, indicating that this variable is mainly affected by BT. Additionally, increases in SS cause a shift in the maximum IVPD value towards higher values, while increases in AF at low BT cause an IVPD increase, and increases in AF at high BT cause a decrease in IVPD. On the other hand, Table 2 reveals that the linear term of BT had the greatest (positive) effect on IVPD, while the linear term of AF did not show a significant effect. Likewise, IVPD was affected by the quadratic term of AF, while the quadratic terms of BT and SS did not show a significant effect. Moreover, the BT-SS and BT-AF interactions were found to positively and negatively affect IVPD, respectively. Various authors have reported that, during the extrusion process, protein denaturation and inactivation of antinutritional factors occur due to certain BT and SS. The enzymatic hydrolysis of proteins improves the IVPD (Zhang et al., 2017). Moreover, amaranth exhibits a low IVPD (< 70 %) compared to blue corn (> 70 %) (Hejazi et al., 2016). The stationary point coordinates were calculated (BT = 123.48 °C, SS = 37.92 rpm, AF = 44.87 %), and it was found that the SS value is outside the experimental range. Additionally, the optimization of a response revealed that the maximum desirable IVPD value (87.2 %) was located at BT = 170 °C, SS = 240 rpm, and AF = 4.24 %.

Optimization

To obtain an optimized extruded expanded snack (OEES), the following initial criteria were applied to the response variables: maximize REI, TPC, TF, AoxA, and IVPD values, and minimize AD and H values. Additionally, the criterion used for the process variables BT and SS was "within range", allowing any value within the experimental range. The optimal combination of process variables obtained was BT = 162 °C, SS = 240 rpm, and AF = 12.67 %. However, we considered that the level of amaranth flour inclusion was too low to improve the snack protein quality. Therefore, a second optimization was performed using the criteria "within range" for the



process variables BT and SS and "maximize" the process variable AF. In this sense, we compared a product with the best characteristics according to the design results (first optimization) and a product with the maximum possible inclusion of amaranth to ensure a better supply of essential amino acids (lysine and tryptophan) without sacrificing the physical characteristics of the OEES (second optimization). The optimal combination of process variables obtained for this second criterion was BT = 170 °C, SS = 240 rpm, and AF = 29.05 %. The individual desirability values obtained for the seven response variables associated with the first optimization (OEES1) were: , , , , , , , and the overall desirability associated with these individual desirabilities was . On the other hand, the individual desirability values associated with these individual desirabilities was . Both overall desirabilities were higher than 0.6 and can be considered acceptable and good.

Table 3 shows the theoretical values obtained from the prediction models with their respective theoretical confidence intervals. When comparing these theoretical values from Table 3 with the experimental values from Table 1, it shows that the theoretical predicted values for REI, TPC, TF, and AoxA, which are desired to be as high as possible, presented acceptable high theoretical values after optimization, even higher predicted theoretical values than the experimental values, except for REI, which showed a slightly lower theoretical value than the maximum experimental value shown in Table 1. Similarly, the AD and H values, which are desired to be as low as possible, had low predicted theoretical values after optimization. This demonstrates that the numerical desirability method of the response surface methodology was adequate to adjust the extrusion process conditions to achieve desirable physical (REI), antioxidant (AoxA), phytochemical (TPC, TF), protein digestibility (IVPD) and texture quality (H and AD) values, allowing them to compete in the market with snacks of similar characteristics. However, a deeper characterization of the optimized snacks will be necessary to validate the potential of functional blue corn and amaranth snacks to positively impact the snack market and consumer health.



Table 3. Predicted mean and confidence intervals for the response variables.

	Response variable	Predicted mean	Lower limit of the predicted interval	Upper limit of the predicted interval	
	REI	2.08	2.01	2.19	
	AD	0.17	0.11	0.22	
	Н	8.16	3.66	12.66	
OEES11	TPC	419.7	381.0	458.4	
	TF	404.8	342.4	467.1	
	AoxA	4747.6	4152.18	5343.02	
	IVPD	73.5	63.65	83.34	
	REI	2.05	1.97	2.14	
	AD	0.20	0.15	0.25	
	Н	9.66	5.58	13.74	
OEES2 ²	TPC	383.5	324.9	442.0	
	TF	613.8	510.3	717.2	
	AoxA	4269.1	3680.94	4857.26	
Ontimized	IVPD	81.20	69.49	92.9	

¹Optimized Expanded Extruded Snack 1, ²Optimized Expanded Extruded Snack 2, REI = Radial Expansion Index, AD = Apparent Density (g/cm³), H = Hardness (N), TPC = Total Phenolic Compounds (mg GAE / 100 g, dw), TF = Total Flavonoids (mg QE / 100 g, dw), AoxA = Antioxidant Activity (μmol TE / 100 g, dw), IVPD = In vitro Protein Digestibility (%).

Conclusions

The optimized healthy snacks made by extrusion from blue corn and amaranth, due to their favorable physical, and textural characteristics, protein digestibility, and antioxidant properties, are a suitable alternative to replace unhealthy snacks that are abundant in the market.



Author Contributions

Work conceptualization: Gutiérrez-Dorado R., Perales-Sánchez J.X.K.; Methodology development: Gutiérrez-Dorado R., Perales-Sánchez J.X.K., Ramos-Ferra C.; software handling: Gutiérrez-Dorado R., Ramos-Ferra C., Félix-Medina J.V., Aguilar-Palazuelos E.; Experimental validation: Ramos-Ferra C.; results analysis: Gutiérrez-Dorado R., Perales-Sánchez J.X.K., Ramos-Ferra C.; Data management: Gutiérrez-Dorado R., Perales-Sánchez J.X.K., Ramos-Ferra C.; Manuscript writing and preparation: Ramos-Ferra C.; Drafting, reviewing, and editing: Gutiérrez-Dorado R., Perales-Sánchez J.X.K., Félix-Medina J.V., Aguilar-Palazuelos E., García-Armenta E.; Project administration: Gutiérrez-Dorado R., Perales-Sánchez J.X.K., Funding acquisition: Gutiérrez-Dorado R., Perales-Sánchez J.X.K. All authors have read and approved the published version.

Funding

This research did not receive external funding.

Acknowledgments

We would like to thank the Bioprocesses and Functional Foods Laboratory staff from the Faculty of Chemical and Biological Sciences at the Autonomous University of Sinaloa for their support. Special thanks to CONHACYT for the scholarship granted to Carlos Francisco Ramos Ferra for his master's studies in food science and technology.

Conflict of Interest

The authors declare no conflict of interest.

References

- Arias-Montes, S., & Aquino, D. (2019). Familia Cactaceae I. Flora del Bajío y de Regiones Adyacentes, 209, 1-290. https://doi.org/10.21829/fb.39.2019.209
- Arias-Montes, S., Gama-López, S., & Guzmán-Cruz, U. (1997) Cactaceae. 1ªed. Flora del Valle de Tehuacán-Cuicatlán. Instituto de Biología. Universidad Nacional Autónoma de México. 14, 1-142.
- Ávila-González, H., González-Gallegos, J. G., López-Enríquez, I. L., Ruacho-González, L., Rubio-Cardoza, J., & Castro-Castro, A. (2019). Inventario de las plantas vasculares y tipos de vegetación del Santuario El Palmito, Sinaloa, México. Botanical Sciences, 97 (4), 789-820. https://doi.org/10.17129/botsci.2356
- Bauer, R. (2003). A synopsis of the tribe Hylocereeae F. Buxb. Cactaceae Systematics Initiatives, 17, 3-63.
- Bravo-Bolaños, O., López-García, J., & Sánchez-González, A. (2020). Structure and floristic composition of the *Quercus* forests of Sanganguey Volcano, Nayarit, Mexico. Botanical Sciences, 98(3), 441-452. https://doi.org/10.17129/botsci.2490



- Bravo-Hollis, H., & Sánchez-Mejorada, H. (1978). Las Cactáceas de México Vol. 1. Universidad Nacional Autónoma de México. México, D.F. 743 pp.
- Comisión Nacional Forestal [CONAFOR]. (2014). Inventario Nacional Forestal y de Suelos. Procedimientos de muestreo. Guadalajara, Jal., México:
- Cruz M, Á., Arias, S., & Terrazas, T. (2016). Molecular phylogeny and taxonomy of the genus Disocactus (Cactaceae), based on the DNA sequences of six chloroplast markers. Willdenowia, 46(1), 145 164. https://dx.doi.org/10.3372/wi.46.46112
- Instituto Nacional de Estadística y Geografía [INEGI]. (2017). Mapa digital de México. Recuperado el 2 de mayo de 2017, a partir de https://www.inegi.org.mx/geo/contenidos/mapadigital/
- Unión Internacional para la Conservación de la Naturaleza [IUCN]. (2024). *The IUCN Red List of Threatened Species. Version 2023-1*. https://www.iucnredlist.org.
- Kimnach, M. (1993). The genus Disocactus. Haseltonia, 1, 95-139.
- Korotkova, N., Borsch, T., & Arias, S. (2017). A phylogenetic framework for the Hylocereeae (Cactaceae) and implications for the circumscription of the genera. Phytotaxa, 327(1), 1-46. https://doi.org/10.11646/phytotaxa.327.1.1
- Cares, R. A., Sáez-Cordovez, C., Valiente-Banuet, A., Medel, R., & Bozzo-Mahan, C. (2018). Frugivory and seed dispersal in the endemic cactus Eulychnia acida: extending the anachronism hypothesis to the Chilean Mediterranean ecosystem. Revista Chilena de Historia Natural, 91, 9. http://dx.doi.org/10.1186/s40693-018-0079-4.
- González-Elizondo, M. S., González-Elizondo, M., Tena-Flores, J. A., Ruacho-González, L., & López-Enríquez, L. (2012). Vegetación de la Sierra Madre Occidental, México: Una Síntesis. Acta Botánica Mexicana, 100, 351-403. https://doi.org/10.21829/abm100.2012.40
- González-Elizondo, M., González-Elizondo, M. S., Retana-Rentería, F. I., Ruacho-González, L. I., López-Enríquez, L. & Tena-Flores, J. A. (2015). Florística de las Cactáceas de Durango. Instituto Politécnico Nacional. Centro Interdisciplinario de Investigación para el Desarrollo Integral Regional-Unidad Durango. Informe final SNIB-CONABIO proyecto No. JF032. México, D. F.
- Guzmán, U., Arias, S. & Dávila, P. (2003). Catálogo de Cactáceas Mexicanas. Universidad Nacional Autónoma de México-Comisión Nacional para el Conocimiento y Uso de la Biodiversidad (UNAM-CONABIO). México, D.F., México. 315 pp.
- Magurran, A. E. (2004). Measuring Biological Diversity. Blackwell Publishing. Victoria, Australia. 256 pp.
- McVaugh, R. (1972). Botanical exploration in Nueva Galicia, Mexico from 1790 to the present time. Contributions from the University of Michigan Herbarium, 9(3-7), 205-357.
- Rzedowski, J. (2006). Vegetación de México. 1ra. ed. digital. Comisión Nacional para el Conocimiento y Uso de la Biodiversidad. México, D.F., México. 504 pp.
- Rzedowski, J., Rzedowski, G. de & Butanda, A. (2009). Los principales colectores de plantas activos en México entre 1700 y 1930. Instituto de Ecología, A.C. y Comisión Nacional para el Conocimiento y Uso de la Biodiversidad. 144 pp.
- Rzedowski, J. (2010). Semblanza Rogers MCvaugh (1909-2009). Acta Botánica Mexicana. 91, 1-7. https://doi.org/10.21829/abm91.2010.285
- Sánchez-Mejorada, H. (1986). Suculentas. In Lot, A. & F. Chiang. Administración y manejo de colecciones, técnicas de recolección y preparación de ejemplares botánicos. (pp 103-111). Ed. Consejo Nacional de la Flora de México.



- Secretaría de Medio Ambiente y Recursos Naturales [SEMARNAT]. (2013). Informe de la situación del medio ambiente. Compendio de estadísticas ambientales. Indicadores clave y de desempeño ambiental. México, D.F. SEMARNAT.
- Téllez-Valdez, O. (1995). Flora, Vegetación y Fitogeografía de Nayarit, México. Tesis de Maestría en Ciencias. Facultad de Ciencias, Universidad Nacional Autónoma de México.
- Téllez V, O. G., Flores, F. A., Martínez, R. R. E., González, F. G., Segura, H. R.I., Ramírez, R. A., Domínguez, M., & Calzada, I. (1995). Flora de la Reserva Ecológica Sierra de San Juan, Nayarit, México. Listados Florísticos de México XII. Instituto de Biología, Universidad Nacional Autónoma de México. México, DF. 50 pp.
- Vega-Aviña, R., Vega-López, I. F., & Delgado-Vargas, F. (2021). Flora Nativa y Naturalizada del Estado de Sinaloa. Universidad Autónoma de Sinaloa. Culiacán, México. 243 pp.
- Véliz-Pérez, M. E. (2008). Las Cactáceas de Guatemala. Unidad de Investigación Herbario BIGU Universidad de San Carlos de Guatemala. San Cristóbal II, Guatemala. 129 pp.
- Villaseñor-Ríos, J. L. (2016). Catálogo de las Plantas Vasculares Nativas de México. Revista Mexicana de Biodiversidad, 87(3), 559-902. https://doi.org/10.1016/j.rmb.2016.06.017